Ukrainian Journal of Physical Optics
ISSUE 2
2025

ANISOTROPY OF ACOUSTO-OPTIC FIGURE OF MERIT IN Tl_3AsS_4 CRYSTALS. ANISOTROPIC DIFFRACTION

O. MYS, M. KOSTYRKO, R. VLOKH

O.G. Vlokh Insitute of Physical Optics, Ivan Franko National University of Lviv

Received: 26.02.2025

Abstract. The anisotropy of the acousto-optic (AO) figure of merit for the case of anisotropic AO diffraction has been analyzed for Tl_3AsS_4 crystals in the principle crystallographic planes. It has been found that the most effective geometries of anisotropic AO Bragg diffraction belong to those that concern interaction with the slowest acoustic wave, i.e., in the *ab* plane with M_2=2020×10^{-15} s^3/kg and the *ca* plane with M_2=1940×10^{-15} s^3/kg. The efficiency of the collinear AO diffraction is highest in the *ca* plane (M_2=141×10^{-15} s^3/kg).

Keywords: acousto-optics, anisotropy, acousto-optic figure of merit, anisotropic diffraction, collinear diffraction, Tl_3AsS_4 crystals
UDC: 535.4, 534.2
DOI: 10.3116/16091833/Ukr.J.Phys.Opt.2025.02080

1. Introduction

The Tl_3AsS_4 crystals are the fangite mineral found in mercury gold deposits in the southern Oquirrh Mountains of Tooele County, Utah, USA and named for Jen-Ho Fang [1]. Thallium arsenic sulfosalt is an orthorhombic crystal that belongs to the point symmetry group mmm. It is characterized by four formula units per cell [1]. The unit cell parameters are equal to a=8.98 Å, b=10.8 Å, and c=8.86 Å [2,3]; i.e., we have the inequality $c < a < b$, which is commonly accepted for non-polar orthorhombic crystals [4]. The density of the crystal is equal to ρ=6200±40 kg/m^3 [2].

The Tl_3AsS_4 crystals are interesting materials from the point of view of their application as acousto-optic (AO) materials. It has been efficiently used in tunable AO filters for the far infrared range. According to Ref. [2], the maximal value of the AO figure of merit reached in the propagation of interacting acoustic and optical waves along principal crystallographic axes is equal to ~800×10^{-15}s^3/kg. In our recent work [5], we have analyzed the anisotropy of the AO figure of merit within the crystallographic planes of Tl_3AsS_4 crystals for the case of isotropic AO diffraction. It has been found that the maximal value of this parameter, equal to 2186×10^{-15} s^3/kg (λ=632.8 nm), is peculiar for the AO interactions with the pure longitudinal acoustic waves (AW) in the *ab* and *bc* planes when the AW propagates along the crystallographic axis *b*. For the anisotropic diffraction the maximal AO figure of merit determined by us for the case in which the interacting waves propagate along the directions close to crystallographic axes is equal to 1990×10^{-15} s^3/kg [6]. This value is reached in the interaction plane *ab* with the transverse AW propagated with the velocity 630 m/s along the *b* axis with polarization parallel to the *c* axis. However, in Ref. [6], the analysis of the anisotropy of the AO figure of merit at the anisotropic diffraction has not been carried out. Therefore, this is the aim of present work.

2. Method of analysis

For further analysis, the main properties of Tl_3AsS_4 crystals should be reminded. The Tl_3AsS_4 crystals are optically biaxial, with the principal refractive indices n_a^g =2.829, n_b^p =2.774, and n_c^m =2.825 at the wavelength λ=632.8 nm [2], and transparent in a broad spectral range (λ=0.6–12 μm [2]). The acute bisector of the optic axes corresponds to the crystallographic axis *b*, while the *ab* plane coincides with the plane of optic axes. The acute angle 2*V* between the optic axes has been measured experimentally at λ=632.8 nm (2*V*=28.46±0.1 deg [7]), which agrees well with the value 29.76 deg calculated following the refractive indices [2]. The elastic stiffness coefficients of Tl_3AsS_4 are equal to C_{11}=(3.19±0.08)×10^{10}, C_{22}=(2.84±0.08)×10^{10}, C_{33}=(3.48±0.19)×10^{10}, C_{12}=(1.62±0.18)×10^{10}, C_{13}=(1.50±0.25)×10^{10}, C_{23}=(1.82±0.20)×10^{10}, C_{44}=(0.25±0.01)×10^{10}, C_{55}=(0.86±0.01)×10^{10}, and C_{66}=(0.89±0.02)×10^{10} N/m^2 [7]. The slowest transverse AW with the velocity 630±6 m/s propagates along the *b* axis with its polarization parallel to the *c* axis. The *a*-axis is the acoustic axis for the transverse AWs, i.e., the velocities of v_{12} = 1196±13 and v_{13} =1176±9 are quite close (in v_{ij} – *i* and *j* indicate the direction of propagation and polarization of AW, respectively) [7]. The elasto-optic (EO) coefficients determined earlier by us at λ=632.8 nm [8] are equal to p_{11}=0.44±0.05, p_{12}=0.32 ±0.05, p_{13}=0.31±0.06, p_{21}=0.45±0.05, p_{22}=0.54±0.07, p_{23}=0.36±0.06, p_{31}=0.28±0.05, p_{32}=0.28±0.05, p_{33}=0.43±0.05, p_{44}=0.08±0.02, p_{55}=0.04±0.02, and p_{66}=0.00±0.03.

The AO figure of merit is determined by the relation:

$$M_2 = \left(n_i^3 n_d^3 p_{eff}^2\right) \Big/ \left(\rho v_{ij}^3\right) , \tag{1}$$

where n_i and n_d are the refractive indices of the incident and diffracted optical waves, p_{eff} - effective elasto-optic coefficient, and ρ - is the density.

Our analysis will consider anisotropic AO interaction in the principle crystallographic planes with the pure transverse (PT) AW. The anisotropic AO interaction cannot be realized in the principle crystallographic planes with quasi-longitudinal (QL) and quasi-transverse (QT) AW since there are no respective EO coefficients to ensure AO coupling. The diffraction angle γ has been changed within 360 deg with the step of 1 deg. The incident angle φ_i has been changed within 0-90 deg with the step of 1 deg. We will consider a upshift (i.e., anti-Stokes) case of AO Bragg diffraction ($k_i + K_{ac} = k_d$ and $\omega_i + \Omega_{ac} = \omega_d$, where k_i, k_d, and K_{ac} are the wavevectors of the incident, diffracted, and acoustic waves, respectively, while ω_i, ω_d, and Ω_{ac} are their frequencies).

2.1 Effective elasto-optic coefficients

Let us consider AO interaction in the *ca* crystallographic plane. The AW propagates under the angle Θ concerning the *a*-axis (Fig. 1a) and is polarized parallel to the *b*-axis. The incident optical wave propagates under the angle φ_i concerning *a*-axis and diffracts under the angle $\varphi_i + \gamma$, where γ is the diffraction angle. The Θ angle is given by the relation:

$$\Theta(\varphi_i + \gamma) = \mathrm{a\,tan}\left\{ \frac{\dfrac{n_a n_c \sin(\varphi_i + \gamma)}{\sqrt{n_a^2 \cos^2(\varphi_i + \gamma) + n_c^2 \sin^2(\varphi_i + \gamma)}} - n_b \sin(\varphi_i)}{\dfrac{n_a n_c \cos(\varphi_i + \gamma)}{\sqrt{n_a^2 \cos^2(\varphi_i + \gamma) + n_c^2 \sin^2(\varphi_i + \gamma)}} - n_b \cos(\varphi_i)} \right\}. \tag{2}$$

The AW induces the deformation tensor components:

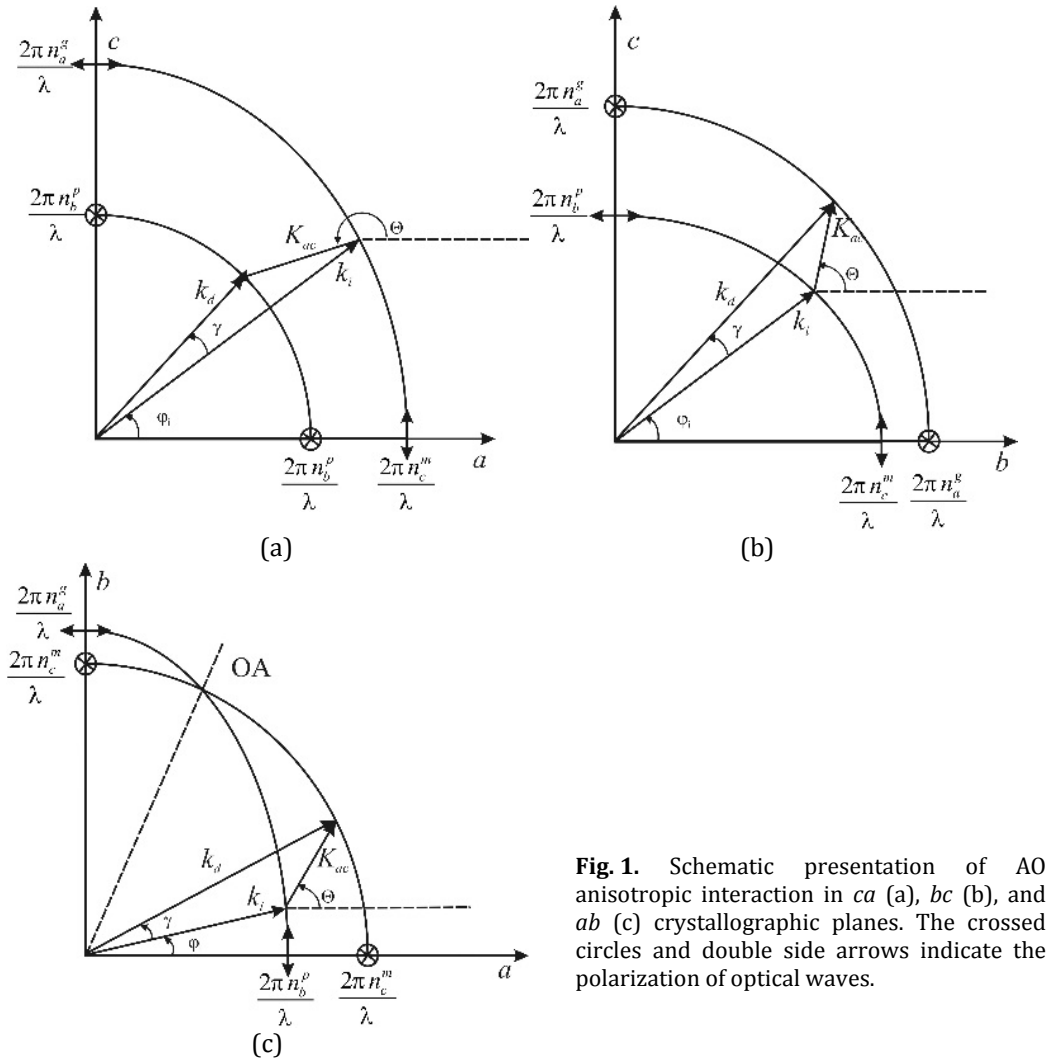

Fig. 1. Schematic presentation of AO anisotropic interaction in *ca* (a), *bc* (b), and *ab* (c) crystallographic planes. The crossed circles and double side arrows indicate the polarization of optical waves.

$$e_6 = \cos(\Theta),\ e_4 = \sin(\Theta), \tag{3}$$

The relation for the effective EO coefficients is as follows:

$$p_{eff} = p_{66}\cos(\Theta)\sin\varphi_i - p_{44}\sin(\Theta)\cos\varphi_i\,. \tag{4}$$

In the *bc* crystallographic plane, the AW propagates under the angle Θ concerning the *b*-axis (Fig. 1b) and is polarized parallel to *a*-axis. Angle φ_i is calculated concerning the *b*-axis. Angle Θ is written as:

$$\Theta(\varphi_i+\gamma) = \mathrm{a}\tan\left\{\frac{\dfrac{n_b n_c \sin(\varphi_i+\gamma)}{\sqrt{n_b^2\cos^2(\varphi_i+\gamma)+n_c^2\sin^2(\varphi_i+\gamma)}} - n_a\sin(\varphi_i)}{\dfrac{n_b n_c \cos(\varphi_i+\gamma)}{\sqrt{n_b^2\cos^2(\varphi_i+\gamma)+n_c^2\sin^2(\varphi_i+\gamma)}} - n_a\cos(\varphi_i)}\right\}. \tag{5}$$

The relation for the effective EO coefficients is as follows:

$$p_{eff} = p_{66}\sin(\Theta)\sin\varphi_i - p_{55}\cos(\Theta)\cos\varphi_i\,. \tag{6}$$

In the *ab* crystallographic plane, the AW propagates under the angle Θ concerning the *a*-axis (Fig. 1c) and is polarized parallel to *c*-axis. Angle φ_i is calculated the concerning *a*-axis. The relation for angle Θ can be written as:

$$\Theta(\varphi_i+\gamma)=\mathrm{a}\tan\left\{\frac{\dfrac{n_b n_c\sin(\varphi_i+\gamma)}{\sqrt{n_b^2\cos^2(\varphi_i+\gamma)+n_c^2\sin^2(\varphi_i+\gamma)}}-n_a\sin(\varphi_i)}{\dfrac{n_b n_c\cos(\varphi_i+\gamma)}{\sqrt{n_b^2\cos^2(\varphi_i+\gamma)+n_c^2\sin^2(\varphi_i+\gamma)}}-n_a\cos(\varphi_i)}\right\}. \quad (7)$$

Since the *ab* plane is the plane of the optical axes, one has to consider the switching of polarization of the optical wave, at the passing of the wavevector through the direction of the optical axes. The polarization switching is caused by the topological defect of optical indicatrix orientation that appears around optical axes in optically biaxial crystals. The strength of this topological defect is equal to ½, which means that the crossection of the optical indicatrix rotates at 180 deg when the tracing angle passes 360 deg around the direction of the optical axis outlet. Therefore one has to consider the region before optical axis ($0<\varphi_i\leq 75$ deg) and after it ($75<\varphi_i\leq 90$ deg) for the incident optical wave. At $0<\varphi_i\leq 75$ deg the incident optical wave is polarized in the *ab* plane, while the diffracted wave is polarized parallel to *c* axis. Then effective EO coefficient is determined as:

$$p_{eff}=p_{55}\sin(\Theta)\cos\varphi_i-p_{44}\sin(\Theta)\sin\varphi_i. \quad (8)$$

When the diffraction angle exceeds 75 deg the diffracted optical wave becomes polarized in *ab* plane. Notice that the diffracted optical wave in this case is polarized in the same way as the incident one despite the anisotropic diffraction occur. However, since the EO tensor component p_{14}, p_{15}, p_{64}, p_{65}, p_{24} and p_{25} are equal to zero for mmm point group of symmetry, this type of diffraction cannot occur.

At $75<\varphi_i\leq 90$ deg the incident optical wave becomes polarized parallel to *c* axis, while the diffracted optical wave is polarized in *ab* plane. Then the effective EO coefficient is determined as:

$$p_{eff}=p_{44}\sin(\Theta)\cos\varphi_i-p_{55}\cos(\Theta)\sin\varphi_i. \quad (9)$$

However when the wavevector of the diffracted wave passes the optical axis $\varphi_i>75$ deg the diffracted optical wave is polarized parallel to *c* axis. In this case the effective EO coefficient includes EO tensor components p_{34} and p_{35} which are equal to zero.

2.2. Acoustic wave velocities

In the *ca* crystallographic plane the AW velocity of PT_1 AW is determined by the relation:

$$\upsilon_{PT}=\sqrt{\frac{C_{66}\cos^2(\Theta)+C_{44}\sin^2(\Theta)}{\rho}}. \quad (10)$$

In the *bc* plane the relation for AW velocity of this wave is as follows:

$$\upsilon_{PT}=\sqrt{\frac{C_{66}\cos^2(\Theta)+C_{55}\sin^2(\Theta)}{\rho}}, \quad (11)$$

and in the *ab* crystallographic plane the respective velocity is determined as:

$$\upsilon_{PT}=\sqrt{\frac{C_{55}\cos^2(\Theta)+C_{44}\sin^2(\Theta)}{\rho}}. \quad (12)$$

3. Results and discussion

The dependencies of the square of effective EO coefficient and AO figure of merit on diffraction angle for different incident angles in *ac* crystallographic plane is presented in Fig. 2. As one can see, the maximal value of the AO figure of merit (1940×10^{-15} s^3/kg) is reached at the propagation of the incident optical wave along *a*-axis and the diffraction angle

equal to ±11 deg. The scheme of this anisotropic type of AO interaction is presented in Fig. 3a. The PT AW at this interaction propagates under an angle of 89.9 deg with respect to the *a*-axis. The frequency of AW is equal to f_a=537 MHz.

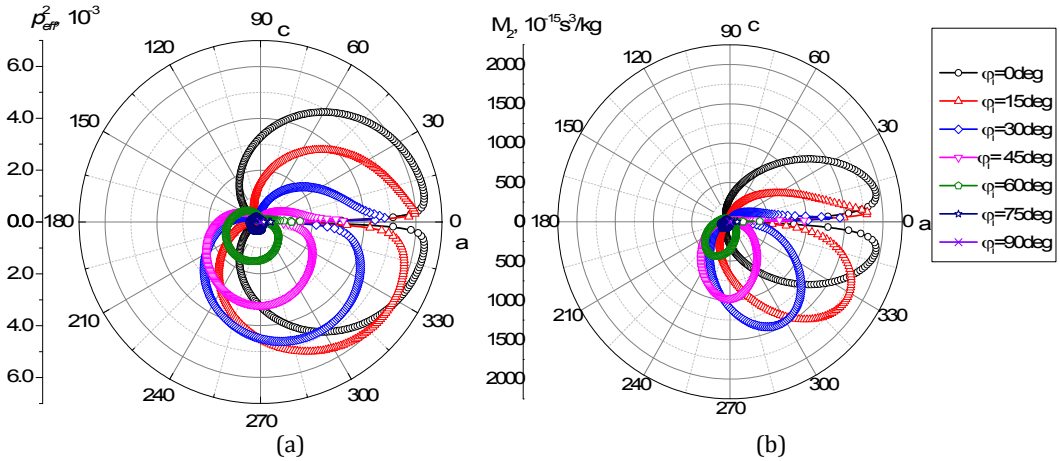

Fig. 2. Dependence of square of effective EO coefficient (a) and AO figure of merit (b) on the diffraction angle γ in the *ac* crystallographic plane for different incident angles φ_i.

Notice that in the *ac* crystallographic plane, the collinear AO diffraction can be realized except φ_i=0 and 180 deg. The maximal value of the AO figure of merit ($141\times10^{-15}s^3/kg$) appears at the angle of incidence equal to φ_i=45 deg (see Fig. 3b). The AW frequency for this type of collinear AO diffraction is equal to 4 GHz. For the case of backward collinear diffraction the AW frequency is as high as 5.64 GHz.

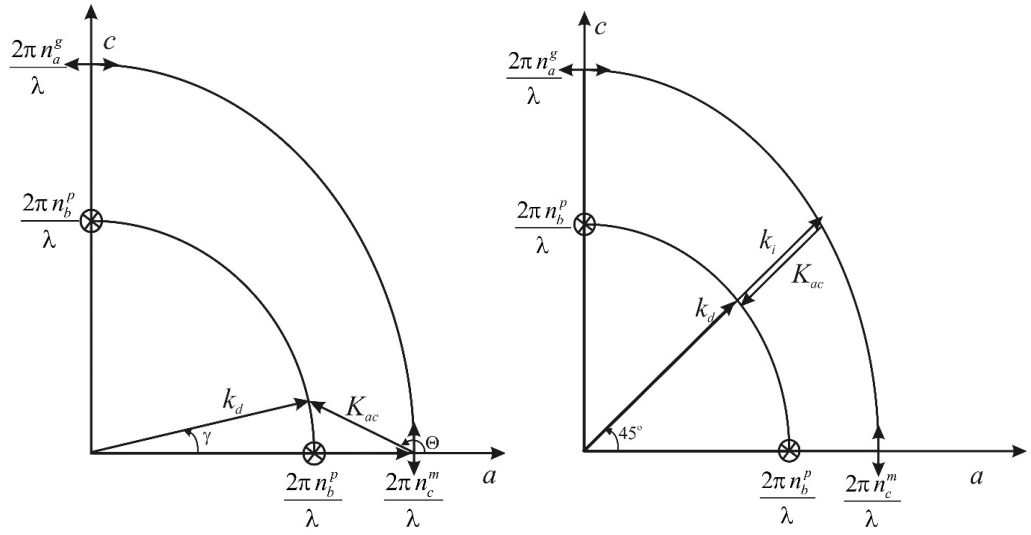

Fig. 3. Scheme of anisotropic (a) and collinear (b) AO interaction in *ca* plane at which maximal values of AO figure of merit are reached. The crossed circles and double side arrows indicate the polarization of optical waves.

In the *bc* crystallographic plane, the maximal value of the AO figure of merit (as well as effective EO coefficient) (see Fig. 4) corresponds to the condition of the angle of incidence φ_i=0 deg and diffraction angle ±1 deg. The AW propagates almost parallel to the *c*-axis with a

velocity equal to 1176 m/s and a frequency of 92 MHz. The AO figure of merit at this geometry of AO interaction (Fig. 5) equals 80×10^{-15}s^3/kg. In the *bc* crystallographic plane, the collinear AO diffraction can be realized except φ_i=0 and 90 deg. The maximal value of the AO figure of merit (19×10^{-15}s^3/kg) appears at the angle of incidence equal to φ_i=45 deg (see Fig. 3b). The AW frequency for this type of collinear AO diffraction is equal to 56 MHz. For the case of backward collinear diffraction the AW frequency is as high as 10 GHz.

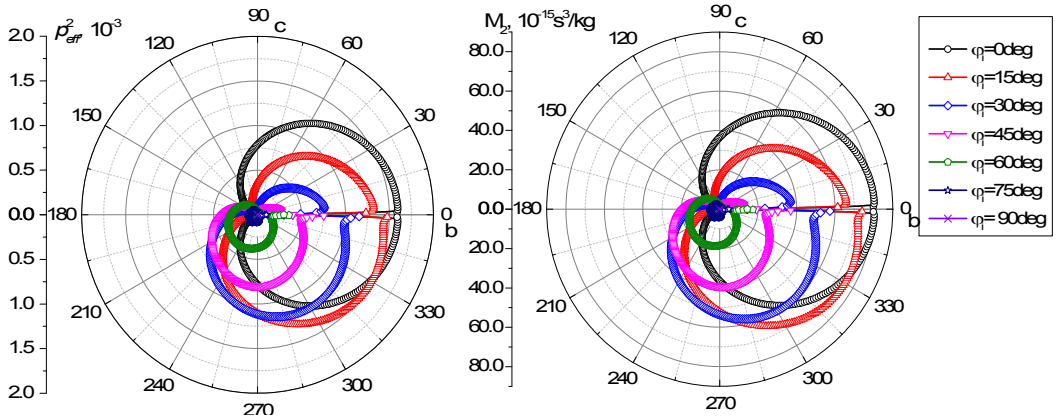

Fig. 4. Dependence of square of effective EO coefficient (a) and AO figure of merit (b) on the diffraction angle γ in the *bc* crystallographic plane for different incident angles φ_i.

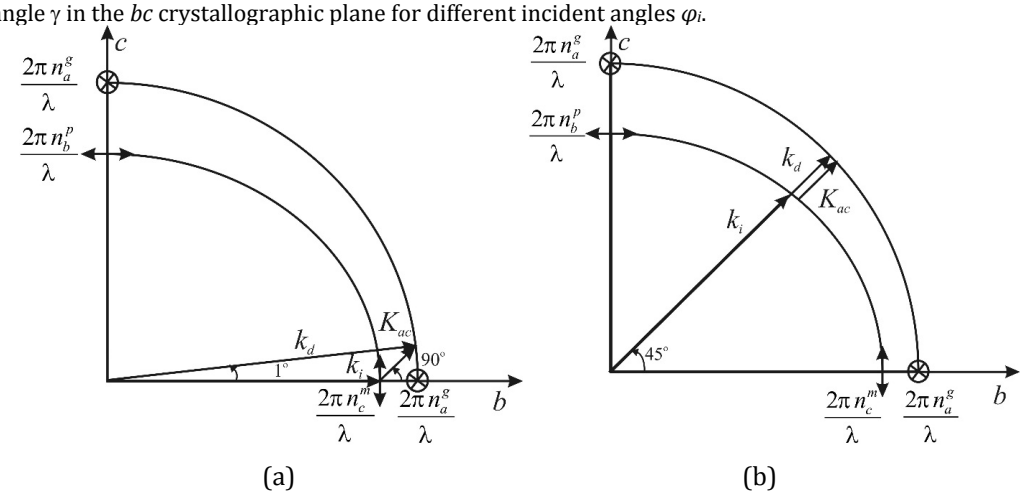

Fig. 5. Scheme of anisotropic (a) and collinear (b) AO interaction in *bc* plane at which maximal values of AO figure of merit are reached. The crossed circles and double side arrows indicate the polarization of optical waves.

The dependencies of effective EO coefficients and AO figure of merit on the diffraction angle in the *ac* plane are presented in Fig. 6. The maximal value of the AO figure of merit is achieved for the conditions of propagation of the incident optical wave along the *a*-axis. In this case, M_2=2020×10^{-15}s^3/kg while the diffraction angle equals ±3 deg (Figs. 6b and 7a). This type of anisotropic diffraction is realized at the frequency of AW, propagated almost along the *b*-axis, equal to 149 MHz. The AO figure of merit at the collinear AO diffraction is equal to 45×10^{-15}s^3/kg under the conditions when three interactive waves propagate under the angle of 60 deg with respect to the *a*-axis (Fig. 7b). The AW frequencies for the forward and backward collinear diffractions are equal to 260 MHz and 5.7 GHz, respectively.

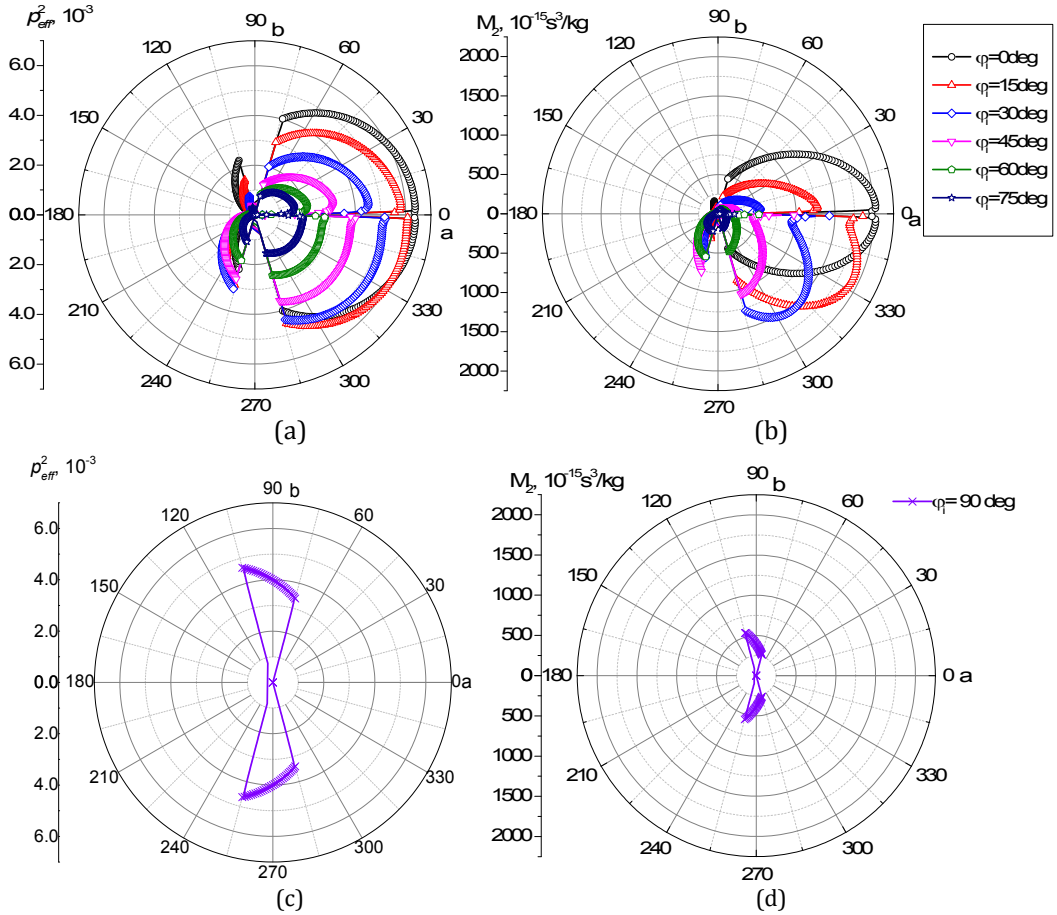

Fig. 6. Dependence of square of effective EO coefficient (a, c) and AO figure of merit (b, d) on the diffraction angle γ in the *ab* crystallographic plane for different incident angles φ_i: 0 deg<φ_i≤75 deg (a,b), 75 deg<φ_i≤90 deg (c,d).

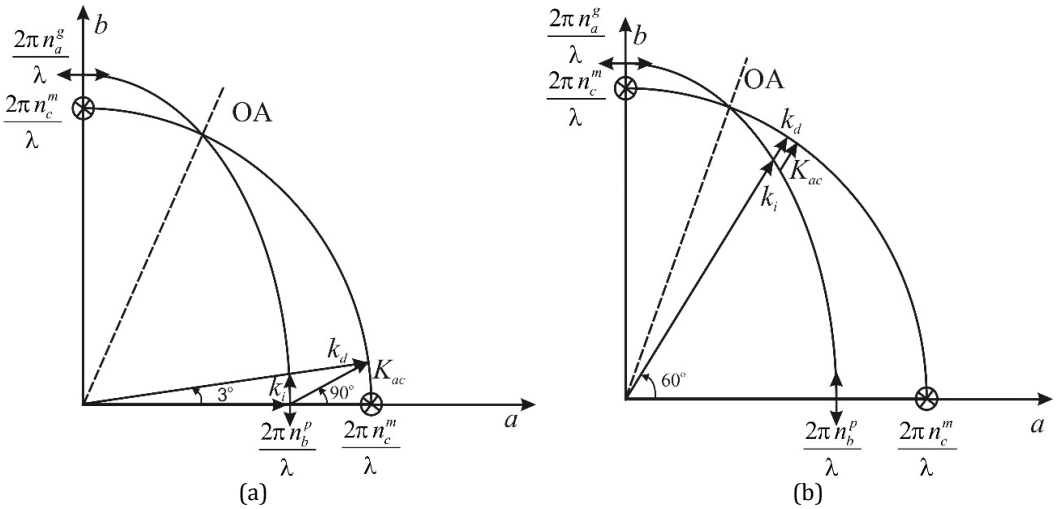

Fig. 7. Scheme of anisotropic (a) and collinear (b) AO interaction in *ab* plane at which maximal values of AO figure of merit are reached. The crossed circles and double side arrows indicate the polarization of optical waves; OA is the direction of the optical axis.

The results of the analysis are combined in Table 1. The most effective geometries of anisotropic AO Bragg diffraction belong to those that concern interaction with the slowest AW, i.e., in the *ab* plane with M_2=2020×10^{-15} s^3/kg and the *ca* plane with M_2=1940×10^{-15} s^3/kg. The efficiency of the collinear AO diffraction is highest in the *ca* plane (M_2=141×10^{-15} s^3/kg). However, the AW frequency for this type of forward diffraction is quite high (4.0 GHz) that is difficult to realize. More preferable is collinear AO diffraction in *ab* plane with M_2=45×10^{-15} s^3/kg and the frequency of AW equal to 260 MHz or in the *bc* plane with M_2=19×10^{-15} s^3/kg and the frequency of AW equal to 56 MHz.

Table 1. Conditions of anisotropic AO diffraction at which maximum values of AO figures of merit are reached.

Diffraction parameters	φ_i, deg	γ, deg	Θ, deg	AW velocity, m/s	f_a, GHz	M_2, 10^{-15} s^3/kg
Interaction plane *ca*						
Tangential Bragg diffraction	0	±11	89.9	631	0.537	1940
Collinear diffraction	45	0* 180**	45* 225**	965	4.0* 5.64**	141
Interaction plane *bc*						
Tangential Bragg diffraction	0	±1	90	1176	0.092	80
Collinear diffraction	45	0* 180**	45* 225**	1186	0.056* 10**	19
Interaction plane *ab*						
Tangential Bragg diffraction	0	±3	90	630	0.149	2020
Collinear diffraction	60	0* 180**	60* 140**	811	0.26* 5.7**	45

* Forward collinear diffraction

** Backward collinear diffraction

4. Conclusions

Summarizing the obtained results, one can suggest that the Tl3AsS4 crystals are efficient AO materials for constructing AO devices based on anisotropic diffraction. This also concerns collinear diffraction. In particular, these crystals possess an AO figure of merit for collinear diffraction comparable with that of the KRS-5 crystal, which can be used as the materials for tunable AO filters for the IR spectral range [9,10]. As stated above, the anisotropic AO interaction cannot be realized in the principle crystallographic planes with QL and QT AW since there are no respective EO coefficients to ensure AO coupling. However, this AO diffraction can be realized out of crystallographic planes due to the involvement of additional components of the EO tensor in the effective EO coefficients. The analysis of this diffraction will be the aim of our forthcoming papers.

References

1. Wilson, J. R., Sen Gupta, P. K., Robinson, P. D., & Criddle, A. J. (1993). Fangite, Tl_3AsS_4, a new thallium arsenic sulfosalt from the Mercur Au deposit, Utah, and revised optical data for gillulyite. *American Mineralogist*, *78*(9-10), 1096-1103.
2. Roland, G. W., Gottlieb, M., & Feichtner, J. D. (1972). Optoacoustic properties of thallium arsenic sulphide, Tl_3AsS_4. *Applied Physics Letters*, *21*(2), 52-54.
3. Goutzoulis, A., Gottlieb, M., Davies, K., & Kun, Z. (1985). Thallium arsenic sulfide acoustooptic Bragg cells. *Applied Optics*, *24*(23), 4183-4188.

4. American National Standards Institute/The Institute of Electrical and Electronics Engineers, Inc. (1987). IEEE Standard on Piezoelectricity. *ANSI/IEEE Std*. 176-1987.
5. Mys, O., Adamenko, D., Krupych, O., & Vlokh, R. (2018). Effect of deviation from purely transverse and longitudinal polarization states of acoustic waves on the anisotropy of acousto-optic figure of merit: the case of Tl_3AsS_4 crystals. *Applied Optics*, *57*(28), 8320-8330.
6. Mys, O., Kryvyy, T., Mytsyk, B., & Vlokh, R. (2018). Acoustooptic figure of merit of Tl_3AsS_4 crystals. The case of acoustic waves propagation along crystallographic axes. *Ukrainian Journal of Physical Optics*, *19* (2), 99-105.
7. Martynyuk-Lototska, I., Kushnirevych, M., Zapeka, B., Krupych, O., Kokhan, O., Pogodin, A., Peresh, E., Mys, O. & Vlokh, R. (2015). Acoustic anisotropy of acoustooptic Tl_3AsS_4 crystals. *Applied Optics*, *54*(6), 1302-1308.
8. Mytsyk, B., Kryvyy, T., Demyanyshyn, N., Mys, O., Martynyuk-Lototska, I., Kokhan, O., & Vlokh, R. (2018). Piezo-, elasto- and acousto-optic properties of Tl_3AsS_4 crystals. *Applied Optics*, *57*(14), 3796-3801.
9. Voloshinov, V. B., Porokhovnichenko, D. L., & Dyakonov, E. A. (2018). Design of far-infrared acousto-optic tunable filter based on backward collinear interaction. *Ultrasonics*, *88*, 207-212.
10. Voloshinov, V. B., Porokhovnichenko, D. L., & Dyakonov, E. A. (2017). Optimization of acousto-optic interaction geometry in KRS-5 crystal for far-infrared applications. *Optical Engineering*, *56*(8), 087102-087102.

O. Mys, M. Kostyrko, R. Vlokh. (2025). Anisotropy of Acousto-Optic Figure of Merit in Tl_3AsS_4 Crystals. Anisotropic Diffraction**.** *Ukrainian Journal of Physical Optics*, *26*(2), 02080 – 02088. doi: 10.3116/16091833/Ukr.J.Phys.Opt.2025.02080

Анотація*. Проаналізовано анізотропію коефіцієнта акустооптичної (АО) якості для випадку анізотропної АО дифракції кристалів Tl_3AsS_4 в основних кристалографічних площинах. Встановлено, що найбільш ефективні геометрії анізотропної Брегґівської АО дифракції належать до тих, які стосуються взаємодії з найповільнішою акустичною хвилею, тобто, в площині ab з $M_2=2020\times10^{-15}$ с^3/кг і в площині ca з $M_2=1940\times10^{-15}$ с^3/кг. Ефективність колінеарної АО дифракції найбільша в площині ca ($M_2=141\times10^{-15}$ с^3/кг).*

Ключові слова*: акустооптика, анізотропія, акустооптична добротність, анізотропна дифракція, колінеарна дифракція, кристали Tl_3AsS_4.*